

# 1 Introduction

Engineering of superconducting magnets is one of the major applications of superconductivity. They are used in various fields of science and engineering. The history of development of superconducting magnets for high energy physics is longer than that for other fields. It started in late 1960s. Although magnets constructed at the beginning of the development had unstable behaviors due to magnetic instability, the construction technique of large superconducting magnets made a great progress owing to the studies of cryogenic stabilization by Stekly[1] and development of multifilamentary strands[2]. At present, in many particle accelerators, superconducting magnets have been developed and used for bending and focusing beams: *Tevatron* (FNAL), *HERA* (DESY), *LEP* (CERN), *TRISTAN* (KEK), *RHIC* (BNL), *LHC* (CERN) and *B-Factory* (KEK).

There are two obvious reasons why superconducting accelerator magnets are developed enthusiastically. One reason is that superconducting magnets allow higher particle energies because of higher magnetic fields compared with normal magnets with iron yokes. While the magnetic fields of normal magnets are generally limited to less than about 2 T(Tesla) due to saturation of iron permeability, superconducting magnets can be excited above magnetic fields of 6T, since the magnetic field of a superconducting magnet is mainly produced by the current in the conductor. Another reason is that it can save operation costs of the machines. For example, a power of 52 MW is needed to excite the machine to a beam energy of 315 GeV in the normal-conducting Super Proton Synchrotron (*SPS*) at CERN, while at HERA the electrical power of 6 MW is sufficient to provide the cooling of the superconducting magnets with a stored proton beam of 820 GeV.

Superconducting magnets have the advantages as mentioned above. However, there are unique difficulties which are not found in normal magnets. A *quench* phenomenon is one of such difficulties. Quench is the transition from the superconducting state to the

normal state, and all superconducting magnets would experience it without exception. Especially, superconducting accelerator magnets are frequently susceptible to quenches due to high current densities compared with superconducting magnets in other fields. Since the volume of an accelerator magnet is required to be reduced as small as possible, the current density of the conductor tends to increase. Table 1.1 shows a comparison with magnets used in various fields. It is clear that the current density of an accelerator magnet is higher than those of magnets in other fields. The problem associated with the increase in current density is the decrease of the stability of a conductor. A *Rutherford cable* used in most superconducting accelerator magnets consists of 20-40 strands of about 1 mm diameter, illustrated in Fig. 1.1(a). The strands have a structure in which a large number of thin filaments are embedded in a copper matrix which provides stability as shown in Fig. 1.1(b). In such a structure, the increase of the amount of superconductor decreases the amount of copper matrix. Therefore, the stability of the cables decreases and quenches occur easily.

The basic process of a quench in an accelerator magnet is as follows: (1) a part of magnet conductor becomes the normal state due to heat by disturbances such as beam losses or frictional energy of a conductor motion, (2) the Joule heat is generated in the normal state region, and (3) the normal state region spreads along the conductor by thermal conduction. In such a quench process, the temperature rise at the part where the quench starts is a serious problem. If the magnet current keeps flowing, the temperature rise will be sufficient to burn the insulation and melt the conductor. In order to avoid these dangers, it is important to estimate the peak temperature of the magnet at the design stage, and necessary to take proper means for protecting them from an excessive temperature rise. The simplified equation for calculating the peak temperature of the magnet,  $T_{max}$ , is given by [3, 4]

$$\int_0^{\infty} I^2(t)dt = A^2 \int_{T_0}^{T_{max}} \frac{C_p(T)}{\rho(T)} dT \equiv U(T_{max}), \quad (1.1)$$

where all the quantities are averaged over the strand cross section;  $I(t)$  is the current,  $t$  is time,  $A$  is the area of conductor cross section,  $T$  is temperature,  $T_0$  is the base temperature,  $C_p(T)$  is the specific heat, and  $\rho(T)$  is the resistivity. The quench process

starts at  $t = 0$ . This equation is derived under an adiabatic condition. Of course, it is a conservative and safer assumption. The value of  $U(T_{max})$  times  $1 \times 10^{-6}$ , called *MIITs*, is one of the important parameters for a magnet design. As an example of calculation, Fig. 1.2 shows *MIITs* using the parameters of the outer cable of a low- $\beta$  insertion quadrupole magnet for LHC[5, 6]. The number of strands of the cable is 30, the strand diameter is 0.737 mm, the magnetic field for this calculation is 5 T, and the copper/superconductor ratio (*Cu/Sc ratio*) is 1.9. As can be seen in Fig. 1.2, *MIITs* is a single function of  $T_{max}$  and an integration of current with time. Therefore, in order to lower  $T_{max}$ , it is necessary to reduce the *MIITs*, that is to say, to decrease the magnet current immediately after quenching. Especially, in a higher region of  $T_{max}$ , this is more important because a little decrease of *MIITs* can decrease the peak temperature largely.

The simplest technique for decreasing magnet current immediately is use of an external dump resistor. Fig. 1.3 shows a simple protection circuit with an external dump resistor, where  $R_q$  is the resistance of the normal region of the magnet,  $L$  is the inductance of the magnet, and  $R_0$  is the resistance of the external dump resistor. When the onset of a quench is detected, the switch is opened and the current flows through the resistor. The equation representing the circuit after quenching is

$$L \frac{dI}{dt} + (R_0 + R_q)I(t) = 0. \quad (1.2)$$

From this equation, the decay constant of the current is given to be  $L/(R_0 + R_q)$ . The larger the denominator becomes, the sooner the magnet current decreases. Since the value  $R_0$  determines the voltage across the magnet, it must be chosen so that the magnet insulation is not broken. Thus the normal resistance  $R_q$  becomes important. As mentioned before, since the normal state region spreads along the conductor, the normal resistance  $R_q$  is a function of spreading velocity of the normal state region, called a *quench propagation velocity*. Therefore, the higher quench propagation velocity is preferable for magnet protection. Fig. 1.4 shows an example of calculation of the influence of the quench propagation velocity on *MIITs*. The cable parameters are the same as in Fig. 1.2. The magnet inductance is 16 mH for the LHC insertion quadrupole model magnet. In order to simplify the calculation,  $R_0$  is set to 0  $\Omega$  and the resistivity

of the cable is assumed to be the average of the values between 4.2 K and 300 K,  $7.5 \times 10^{-9} \Omega \text{m}$ . It is clear from Fig. 1.4 that MIITs decreases with increasing quench propagation velocity.

The basic equation for quench propagation is one dimensional thermal equilibrium equation given by[3]

$$\frac{\partial}{\partial x} \left( \kappa(T) \frac{\partial T}{\partial x} \right) + g(I, T) - \frac{P}{A} q_h = C_p(T) \frac{\partial T}{\partial t}, \quad (1.3)$$

where  $\kappa(T)$  is the thermal conductivity of the cable,  $x$  is the longitudinal position,  $g(I, T)$  is the Joule heat generation in the cable per unit length,  $P$  is the cooled perimeter, and  $q_h$  is the heat transfer to coolant, liquid helium in general. For a single strand cable, the quench propagation velocity can be calculated with some accuracy by considering the appropriate material properties and cooling effects for Eq. (1.3)[7]-[16]. However, in a multi-strand cable, we have some reports that the quench propagation velocities are higher than the velocities predicted by thermal propagation theories[17, 18]. The reason for this effect is considered due to the fact that the quench propagation velocities are influenced with *current redistribution*, namely the current commutation between strands [19].

In the case of a multi-strand cable made of insulated strands with CuNi matrix, an abnormally high quench propagation velocity has been observed. This phenomenon is called *fast quench*[20]-[23]. When a local normal zone is produced in a strand, its current transfers to the neighboring strands through the termination of the cable where all the strands are connected electrically. Then, the successive current redistribution accelerates the elongation of the normal zone. On the contrary, in the case of a multi-strand cable made of non-insulated strands, like a Rutherford cable, there are only a few reports describing that the quench propagation velocities in practical magnets have been measured and that the relation between the quench propagation velocity and the current redistribution has been indicated[17, 24, 25]. The reason for this is that it is difficult to measure a local current redistribution in the cable made of non-insulated strands and to consider such relation experimentally.

The main purpose of the present study is to measure the local current redistribution

in a multi-strand cable made of non-insulated strands, and to discuss the influence of the current redistribution on the quench propagation velocity. The cable used in our tests is an eight-strand Rutherford cable wrapped with polyimide tape for cable insulation. A technique utilizing *pickup coils* was adopted for measurements of the local current redistribution in the cable. The quench tests were performed for the three kinds of cables having three different electrical conductance between strands. Numerical simulations of quench propagation processes in a two-parallel strand model were performed, and the simulation results were compared with experimental results. In addition, the quench propagation velocities of the cable without polyimide tape were also measured, and it was examined how the quench propagation velocity was changed by the influence of polyimide tape on cooling conditions of the cable.

In Chapter 2, the methods and results of the Rutherford cable tests are presented. The apparatuses, especially pickup coils, are explained. Then the measured data of the quench propagation velocity and the current redistribution are shown. Chapter 3 addresses the measurement of the quench propagation velocity in a single strand cable. A numerical model and results are described in Chapter 4. Discussion is given in Chapter 5. Finally, Chapter 6 gives the conclusions.

Table 1.1: Features of superconducting magnets used in various fields.

	Magnetically levitate train	Nuclear fusion LCT coil	Nuclear fusion pulse coil	Particle accelerator
Coil shape	Race track coil impregnated	D shape double pancake	Solenoid double pancake	Shell type dipole coil
Max. field	4.7 T	8.0 T	6.4 T	5.5 T
Current density	183 A/mm <sup>2</sup>	26.6 A/mm <sup>2</sup>	30.4 A/mm <sup>2</sup>	330 A/mm <sup>2</sup>
Current	700 A	10220 A	5500 A	4870 A
Stored energy	522 kJ	104000 kJ	3890 kJ	300 kJ

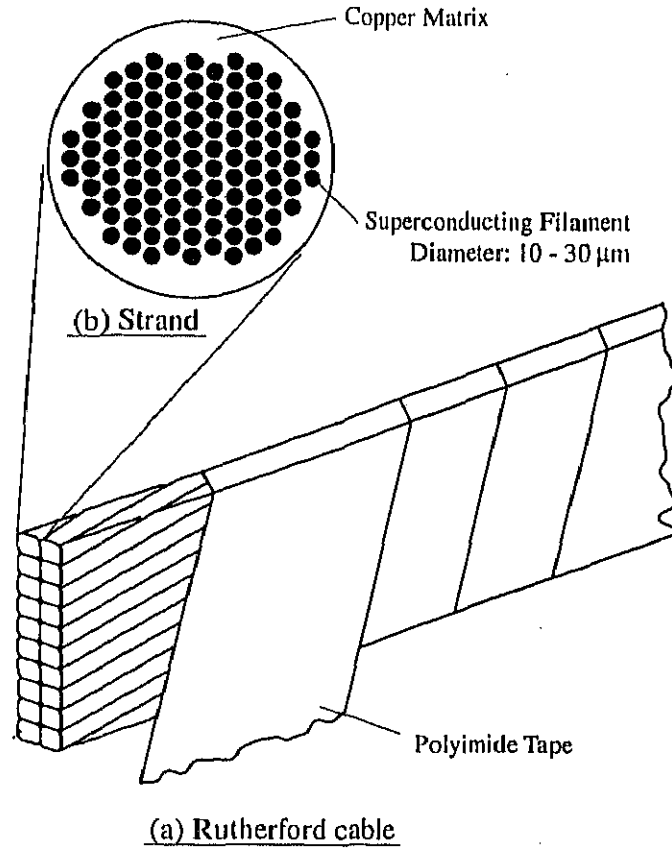


Fig. 1.1: Schematic view of a Rutherford cable and a strand cross section.

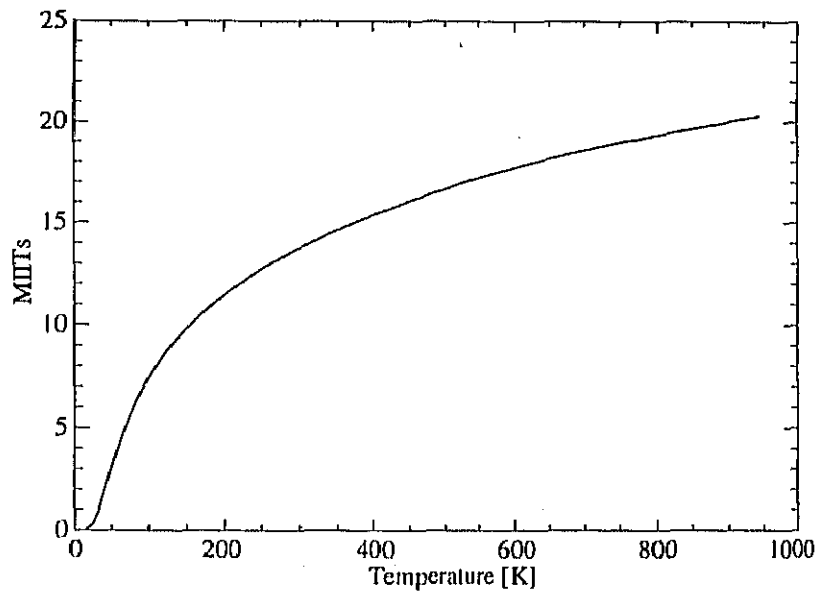


Fig. 1.2: Example of MIITs calculation. The parameters are those of the outer cable parameters for LHC insertion quadrupole magnets.

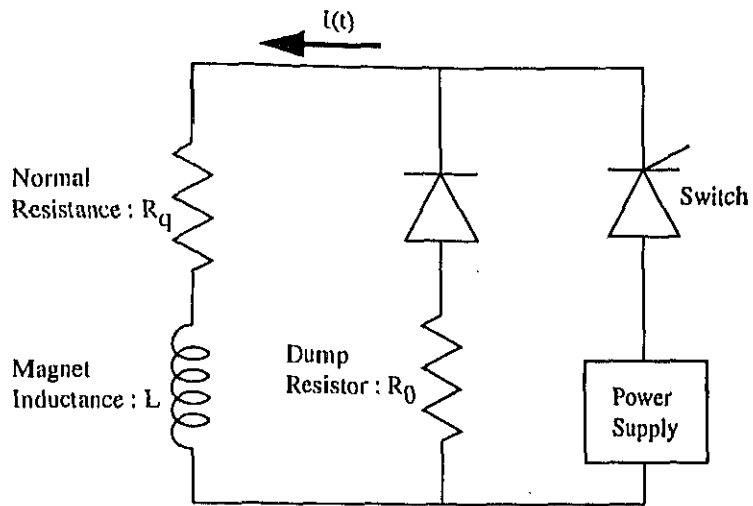


Fig. 1.3: Simple protection circuit with an external dump resistor.

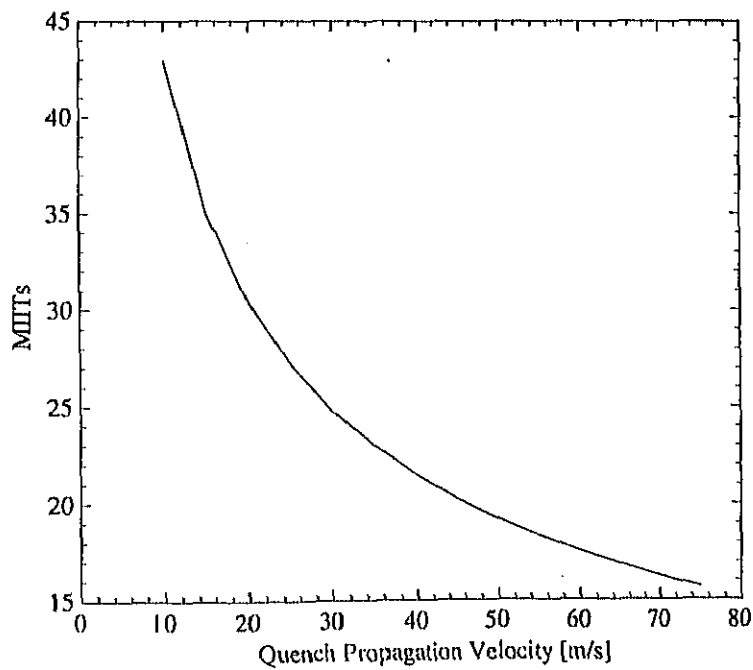


Fig. 1.4: Example of calculated MITs as a function of the quench propagation velocity.